Ultraprecision intersatellite laser interferometry

View the article online for updates and enhancements.

Topical Review

Ultraprecision intersatellite laser interferometry

Min Ming[2], Yingxin Luo[1], Yu-Rong Liang[2], Jing-Yi Zhang[1], Hui-Zong Duan[1], Hao Yan[1], Yuan-Ze Jiang[2], Ling-Feng Lu[1], Qin Xiao[1], Zebing Zhou[2] and Hsien-Chi Yeh[1,3] (iD)

[1] Tianqin Research Center for Gravitational Physics and School of Physics and Astronomy, Sun Yat-sen University (Zhuhai Campus), Zhuhai 519082, People's Republic of China
[2] MOE Key Laboratory of Fundamental Physical Quantities Measurement & Hubei Key Laboratory of Gravitation and Quantum Physics, PGMF and School of Physics, Huazhong University of Science and Technology, Wuhan 430074, People's Republic of China

E-mail: yexianji@mail.sysu.edu.cn

CrossMark

Abstract

Precision measurement tools are compulsory to reduce measurement errors or machining errors in the processes of calibration and manufacturing. The laser interferometer is one of the most important measurement tools invented in the 20th century. Today, it is commonly used in ultraprecision machining and manufacturing, ultraprecision positioning control, and many noncontact optical sensing technologies. So far, the state-of-the-art laser interferometers are the ground-based gravitational-wave detectors, e.g. the Laser Interferometer Gravitational-wave Observatory (LIGO). The LIGO has reached the measurement quantum limit, and some quantum technologies with squeezed light are currently being tested in order to further decompress the noise level. In this paper, we focus on the laser interferometry developed for space-based gravitational-wave detection. The basic working principle and the current status of the key technologies of intersatellite laser interferometry are introduced and discussed in detail. The launch and operation of these large-scale, gravitational-wave detectors based on space-based laser interferometry is proposed for the 2030s.

Keywords: laser interferometry, gravitational-wave detection, inter-satellite laser ranging, transponder laser interferometer

(Some figures may appear in colour only in the online journal)

1. Introduction

A manufacturing system with closed-loop feedback control can reach a very low manufacturing error. In principle, the ultimate manufacturing error is determined by the precision of the measurement device implemented in the feedback control loop. The development of wafer stepper is a good example to demonstrate the significance of a precision measurement system to ultraprecision manufacturing. As we know, the manufacturing of wafer lithography demands higher precision and larger size, the laser interferometers with nanometer-level precision are currently used in the wafer steppers for semiconductor manufacturing.

As one of the most important physical experiments of the 19th century, the Michelson–Morley experiment used an optical interferometer to reveal the truth of the constant speed of light in a vacuum. The Michelson interferometer was well known then and used in many fields of science and

engineering. The laser, invented in the 1960s, significantly enhanced the coherence of light so that the laser interferometer became a most promising measurement tool utilized in many applications for various purposes.

The instruments based on laser interferometry measure specific physical interactions that can induce changes to the optical path length along the arm lengths of an interferometer. For example, the Laser Interferometer Gravitational-wave Observatory (LIGO) [1], built in Hanford Washington and in Livingston, can detect an optical path length difference between two orthogonal interferometer arms with an arm length of 4 km, even down to 10^{-18} m, caused by the gravitational waves passing by. These ground-based gravitational-wave detectors open a totally new window for observing the universe. However, their frequency band of detection is constrained to be above 10 Hz, which is limited mainly by seismic noise and gravitational gradient noise. In order to extend the detection frequency band down to 0.1 mHz, a laser interferometer with an arm length of $10^5 \sim 10^6$ km must be constructed because the gravitational-wave detector is in the most sensitive state when the characteristic length of a laser interferometer (i.e. arm length) has the same scale as the wavelengths of the gravitational waves detected. With this background, the Laser Interferometer Space Antenna (LISA) mission [2] was proposed and developed for more than 20 years and was selected as the third largest project (L3-project) of the Cosmic Vision of the European Space Agency, with a launch planned for the early 2030s.

The LISA has a solar orbit in which three satellites form an equilateral triangle constellation with intersatellite distances of 250 million km. Laser links between two satellites must be made, and at least two laser links are required to build up a laser interferometer. Taking the smallest strength of detected gravitational waves into account, the noise level of an intersatellite laser interferometer must be down to about 10 pm/Hz$^{1/2}$ over a frequency band ranging from 0.1 Hz to 0.1 mHz. In addition to the LISA, spaceborne gravitational-wave detection missions, such as the Astrodynamical Space Test of Relativity using Optical Devices optimized for Gravitational Wave (ASTROD-GW) detection [3], TianQin [4], and Taiji [5], were also proposed based on the same working principle.

The ASTROD-GW is a highly challenging mission in which three spacecraft, orbiting near Sun-Earth Lagrange points, L3, L4, and L5, constitute a 2.6×10^8 km arm length interferometer with a sensitivity of 1 nm/Hz$^{1/2}$. The TianQin uses a geocentric orbit at an altitude of 10^5 km to set up an interferometric gravitational-wave antenna with arm lengths of 1.7×10^5 km. The target sensitivity of the TianQin mission is 1 pm/Hz$^{1/2}$. The mission concept of the Taiji is almost the same as that of the LISA but uses a longer arm length of 300 million km. DECi-hertz Interferometer GW Observatory (DECIGO) [6] was proposed to fill the observation gap between the LISA and the LIGO. Its working principle, based on the Fabry–Pérot (FP) resonance method with a 1000 km cavity length (i.e. intersatellite distance), is different from the other space-based missions.

It is worth pointing out that the laser interferometry of space-based gravitational-wave detection is based on quite a different principle from that of a ground-based one. The ground-based gravitational-wave detector is schematically a Michelson interferometer with FP cavities that can enhance the gravitational-wave signals. The space-based gravitational-wave detector implements transponder-type interferometry since the light power received by a spacecraft becomes very weak due to a long intersatellite propagating distance and an unavoidable laser beam divergence angle. That is, the ground-based detector is basically one Michelson interferometer with problems with reflection of strong light power. In contrast, the space-based detector consists of (at minimum) two transponder interferometers with problems with weak light power received. A detailed analysis is presented in section 3.2.

To give a brief introduction to laser interferometry of gravitational-wave detection in space, figure 1 shows a schematic diagram of the intersatellite transponder interferometer. The frequency-stabilized and power-stabilized neodymium-doped yttrium aluminum garnet (Nd:YAG) laser, known as the master laser, provides a highly coherent light source to meet the needs of interference between the local laser light and the received light. The intersatellite laser beam pointing control system is in charge of acquisition and accurate pointing of the intersatellite laser beams. As the laser light emitting from the master satellite passes through intersatellite space and arrives at the slave satellite, the optical phase-locking system locks the phase of the slave laser to that of the weak light received. Then the slave laser light points and propagates back to the master satellite. Since the information on the length of the round-trip optical path is contained in the phase of the weak light received by the master satellite, the precision phasemeter can obtain this information by measuring the phase difference between the master laser light and the received light. This is the basic principle of transponder laser interferometry.

According to the above description, the key subsystems of the intersatellite laser interferometer for spaceborne gravitational-wave detection include the space-qualified, frequency-stabilized laser; the weak-light phase-locked loop; and the intersatellite beam pointing control system. We introduce the laser frequency stabilization system in section 2. Ultraprecision phase measurement and weak-light phase locking are presented in section 3. The intersatellite laser beam pointing control is discussed in section 4.

2. Frequency stabilization of space-qualified laser

Laser frequency (or wavelength) is the standard scale of displacement measurement for laser interferometry, so the stability of the laser frequency directly influences measurement precision, especially for interferometers with unequal arm length. The typical arm length of a space-based laser interferometer is the intersatellite distance, ranging from a few hundred thousand to millions of kilometers. In these cases, the unequal arm length of the interferometer is an unavoidable problem; and the laser frequency noise becomes a critical issue. Therefore, a highly stable, space-qualified laser must be one of the most important payloads for space missions with intersatellite laser interferometry. In the following sections, we discuss the
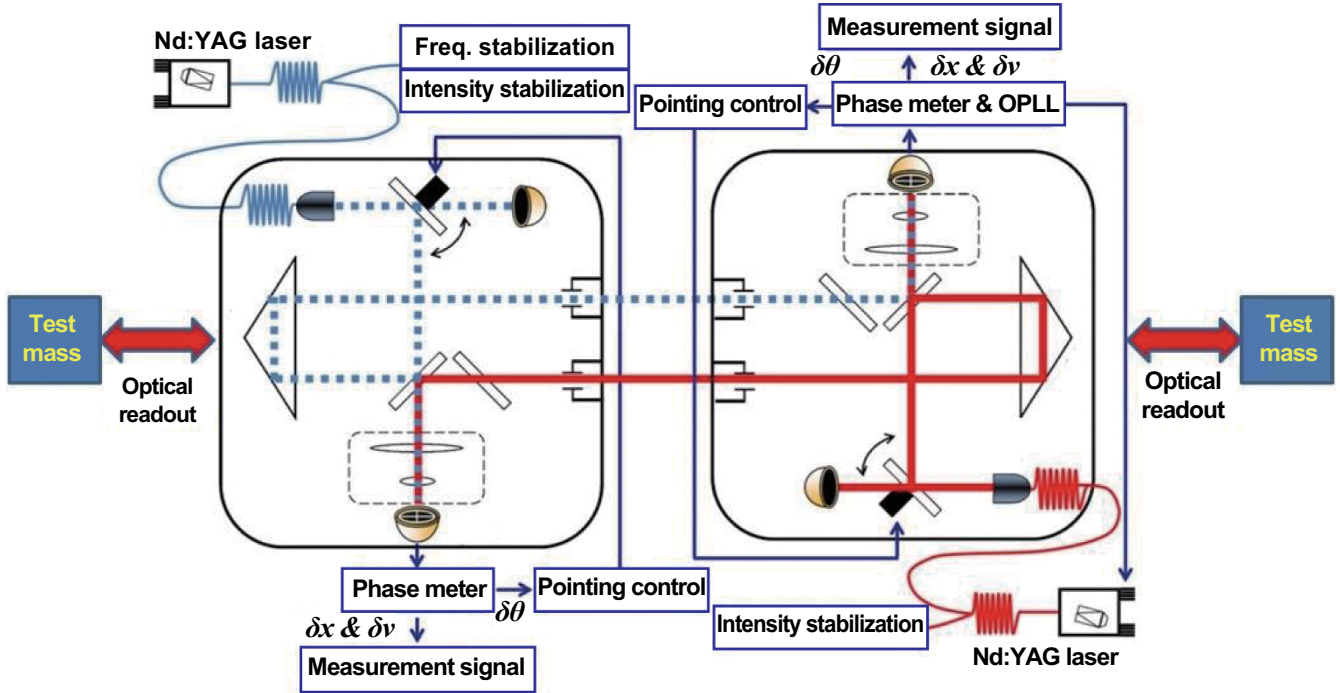
Figure 1. The schematic diagram of the intersatellite laser interferometer used for gravitational-wave detection in space. The left and right optical systems are mounted within the master satellite and the slave satellite, respectively. For the master satellite, the signal from quadrant photodetector is sent to phasemeter that can generates two kinds of output signal. The first are the misalignment angles of local laser beam, $\delta\theta$, for intersatellite laser beam pointing control. The second are the intersatellite relative speed and displacement, δx and δv, for science data recording. For the slave satellite, the working process is similar to the master satellite, except that the output signals of phasemeter must be sent to optical phase-locked loop (OPLL) for weak-light phase locking. Two test masses are protected and locating at the center of accelerometers by using drag-free control.

working principles, requirements, and current research status of space-qualified, ultrastable laser systems.

2.1. Basics on stability of laser

Precise measurement of relative change in the distance between two spacecraft Δd using a laser metrology system is typically achieved by measuring the optical phase change $\Delta\varphi$ of the laser beam propagating along the line of sight of two spacecraft, which is expressed by

$$\Delta d = \lambda \frac{\Delta\varphi}{2\pi} = \frac{c}{v}\frac{\Delta\varphi}{2\pi}, \qquad (1)$$

where λ and ν are the wavelength and frequency of the laser, and c is the velocity of light. According to equation (1), laser frequency fluctuation is one of the sources of noise measurement. The frequency instability of a laser can be characterized by the linewidth, the Allan variance in the time domain, and the power spectral density (or amplitude spectral density) in the frequency domain [7, 8]. The laser linewidth is a measurement of the frequency resolution in spectroscopy. A narrow linewidth represents good monochromaticity and a highly temporal coherence in laser interferometers. The Allan variance, describing the mean value of the momentary relative frequency fluctuation averaged over a time interval, characterizes the temporal stability of laser frequency. The power spectral density (PSD) of laser frequency noise is the Fourier transform of the square of the laser frequency noise. A more commonly used description is its square root. The amplitude spectral density (ASD) characterizes the amplitude distribution of frequency noise with the unit $Hz/Hz^{1/2}$.

For laser interferometry, the spectral density is more advantageous and informative for indicating the laser frequency stability because the scientific target signals are expected to be within a specific frequency band of interest. The total noise measurement can be deduced from the laser frequency noise spectral density by integrating the spectral density within the frequency band of interest.

For an interferometer with unequal arm length L, the displacement measurement error caused by the laser frequency fluctuation can be expressed as,

$$\frac{\Delta d}{L} = \frac{\Delta v}{v}. \qquad (2)$$

2.2. Typical requirements of laser systems

For space-based laser interferometry, a laser with a 1064 nm wavelength is preferred because of the low absorption of the space medium at this wavelength through the intersatellite propagation. High power output is essential for adequate received signal light power at the remote spacecraft in order to reduce the shot noise of interference measurement. In addition

to these two issues, the maturity of a frequency-stabilized laser system must also be taken into account.

The interferometer of the LISA has arm lengths of $2.5 \sim 3 \times 10^9$ m [9]. The required frequency noise of the laser is 30 Hz/Hz$^{1/2}$ from 10 mHz to 1 Hz at a prestabilized state [10] by means of the Pound–Drever–Hall (PDH) method. The laser frequency noise is then further suppressed successively by using the arm-locking technique [11] and time delay interferometry (TDI) [12] to a level of μHz/Hz$^{1/2}$, which arises from the requirement for measurement noise of 10 pm/Hz$^{1/2}$ with 1% relative arm length variation. The residual intensity noise (RIN) of the laser in the LISA should be better than 3×10^{-8}/Hz$^{1/2}$ at the beat frequency and twice the beat frequency and $<2 \times 10^{-4}$/Hz$^{1/2}$ from 0.1 mHz to 1 Hz as well [10]. The latter requirement is for reducing light pressure fluctuation applied on the test masses during measuring of the position of the test mass by optical readout.

The TianQin is also a space-based gravitational-wave detection mission, having a nearly equilateral triangle constellation of three geocentric orbiting spacecraft that are about 1.7×10^5 km away from each other. The laser frequency noise is required to be less than 10 Hz/Hz$^{1/2}$ at 10 mHz after laser frequency prestabilization and then is further suppressed by TDI to a level of 0.1 mHz/Hz$^{1/2}$ to meet the requirement for the measurement noise of 0.5 pm/Hz$^{1/2}$ with 1% arm length mismatch ($\approx$2000 km).

2.3. Space-qualified lasers

Space-qualified lasers must meet the following requirements: (1) the size, weight, and power consumption must be constrained; in principle, the smaller the better; (2) the laser system must be qualified by mechanical, thermal, electromagnetic interference (EMI), and high-energy radiation compatibility tests; (3) all operations of the laser must be automatic onboard; and (4) the laser must be reliable without failure or obvious degradation during the designed lifetime of the space missions.

An Nd:YAG solid-state laser with nonplanar ring oscillator (NPRO) structure [13] and 1064 nm wavelength has been tested for reliability in terms of intrinsic frequency and intensity stability, mechanical robustness, power efficiency, and large tunable frequency range. Space-qualified Nd:YAG NPRO lasers have been developed during the last decades and are commercially available. These lasers have passed all of the qualification tests and have operated successfully in space for the laser communication terminals of TerraSAR [14, 15], the LISA Technology Package of LISA Pathfinder (LPF) [16], and the first intersatellite laser interferometer of Gravity Recovery And Climate Experiment–Follow On mission (GRACE-FO) [17].

Up to a few watts of laser power is required for the application of gravitational-wave detection in space, e.g. LISA and TianQin (see table 1). Promising solutions for generating high laser power of up to 4 W has been realized, including a stand-alone NPRO laser with special mechanical and pumping designs and a master oscillator fiber amplifier (MOFA) configuration that is based on the high-power fiber amplifier seeded

by a low-power stabilized master laser oscillator [18], shown in figure 2.

A fiber-based laser is also suitable for space applications due to its robustness and compactness. The suitability of a commercial Yb-doped distributed feedback (DFB) fiber laser and its amplifier system emitting 1 W of power for the LISA mission has been proposed [19, 20]. Following that, a fiber ring laser that has a comparable free-running frequency noise and a smaller RIN, compared to a Nd:YAG NPRO laser at a low frequency band, was developed for the LISA mission [21]. This fiber ring laser can achieve a faster frequency tuning (up to 10 MHz of bandwidth) than commercial DFB or distributed Bragg reflector (DBR) lasers by using an intracavity phase modulator [22]. Although these Yb fiber lasers perform comparably to Nd:YAG NPRO lasers at a low frequency band, they all show a large RIN peak around 1 MHz due to their typical relaxation oscillation, which could affect the heterodyne interferometry near this frequency.

Recently, the planar-waveguide external cavity diode laser (PW-ECL) has become another promising candidate for a space-qualified master laser because of advantages that include lower cost, less consumption, and more robust design of the butterfly package, as well as better stability compared to other lasers. The PW-ECL laser, which consists of a semiconductor gain chip and a Bragg reflector laser cavity on the planar waveguide, was commercially available for the telecom C-band (around a wavelength of 1550 nm). Its suitability for precision measurements in space has been studied [23, 24]. A 1064 nm version of the commercial PW-ECL laser was successfully built, and a full MOFA system with 2.5 W of output power has shown good stability and reliability results for the LISA mission [25].

A long lifetime is also a critical requirement for a space-qualified laser system, which depends on the reliability of pumping diodes for both the seed laser and fiber amplifier. A highly reliable laser diode pumping unit should enable a steady output of power, good hermetical performance, and redundancy. In addition, compact size, robust mechanical structure, and flexible electrical and optical interfaces are also needed for a space-qualified pumping diode. Over the last two decades, space-qualified pumping modules based on multiple bars or arrays of laser diodes with fiber-coupled, high-power output have been developed [26]; and a 10 W diode pumping module with a reliability of 0.9998 over a ten-year lifetime has been reported [27].

### 2.4. Schemes of laser frequency stabilization in space

A laser frequency stabilization system consists of a frequency-tunable laser, an ultrastable frequency reference, a feedback control electronic system, and compulsory optical and electrical links between the laser and frequency reference.

The PDH technique, invented in 1983 [28], has become the most popular method for laser frequency stabilization by means of locking it to the resonance frequency of an ultrastable FP cavity. The resonances of an FP cavity occur when the roundtrip distance is an integer multiple of laser wavelength,

Table 1. Technical specifications of laser required for various space missions.

Parameter	Science missions			
	GRACE-FO	NGGM	LISA	TianQin
Wavelength (nm)	1064 nm	1064 nm	1064 nm	1064 nm
Power	25 mW	500 Mw	2 W	4 W
RIN (1/Hz$^{1/2}$)	—	3×10^{-8} (at fb/2fb)	2×10^{-4} (0.1 mHz–1 Hz) 3×10^{-8} (at fb/2fb)	2×10^{-4} (1 mHz–1 Hz)
Lifetime	5 years	10 years	5 years	5 years
Frequency stability	30 Hz/Hz$^{1/2}$ (@0.1 Hz)	20 Hz/Hz$^{1/2}$ (@0.1 Hz)	30 Hz/Hz$^{1/2}$ (@10 mHz)	10 Hz/Hz$^{1/2}$ (@10 mHz)

GRACE-FO refers to gravity recovery and climate experiment–follow on mission; NGGM refers to next generation gravity mission.
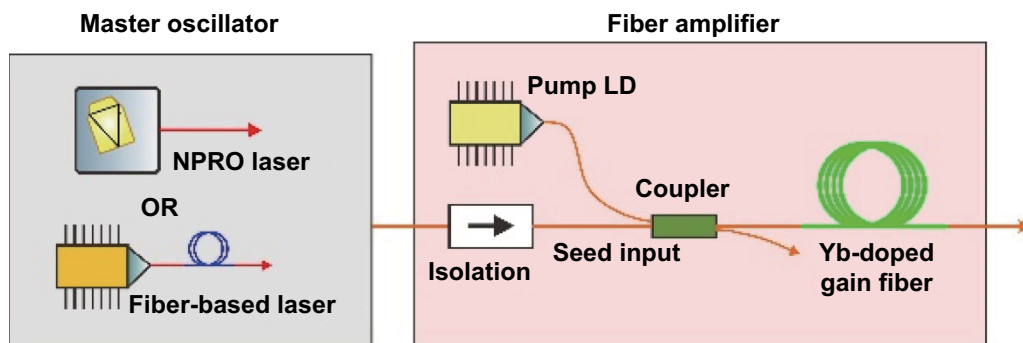
Figure 2. Typical structure of a high-power laser with a MOFA configuration.

and the linewidth of resonance is represented by the cavity finesse that is determined by the reflectivity of cavity mirrors.

Figure 3(a) shows a basic setup for the PDH laser frequency stabilization, in which the electro-optic phase modulation (EOM) is used to produce a pair of Bessel sidebands with equal amplitude and opposite phase on both sides of the laser frequency before they are incident into the FP cavity. When the laser frequency is near the cavity resonance frequency, the signals reflected from the cavity's front mirror form an asymmetric dispersion curve after demodulation by a mixer, as shown in figure 3(b). This is used as the error signal for feedback control of the laser frequency. We will skip the detailed working principle and theoretical analysis about the PDH method. For readers who are interested, please refer to [28, 29].

An ultrastable reference cavity for space applications usually features a high-symmetric geometry and a rigid mounting design for the purpose of acceleration and orientation insensitivity. Moreover, the rigidly mounted optics to maintain a steady mode-matching efficiency between the laser and a certain transverse electromagnetic (TEM) mode of the FP cavity is necessary, as illustrated in figure 3(a).

The space-qualified PDH laser stabilization system for the GRACE-FO mission was developed by the Jet Propulsion Laboratory (JPL) [30] with a high-finesse, tapered structure commercial cavity, a mode-matching optical bench, and a fiber-based optical layout for phase modulation. A frequency stability of 30 Hz/Hz$^{1/2}$ at 0.01 Hz was achieved (shown as a solid black line in figure 4). This system was launched and is working successfully for the GRACE-FO mission [17].

The high stability laser (HSL) system for the next generation gravity mission (NGGM) has been established by the National Physical Laboratory (NPL) [31] and has achieved a laser frequency stability of better than 20 Hz/Hz$^{1/2}$ at a frequency above 0.01 Hz, shown as the solid blue line in figure 4. This system is based on the PDH scheme with an ultrastable cubic cavity mounted symmetrically in a tetrahedral configuration inside a compact vacuum chamber [38].

To meet the needs of the TianQin mission and the next generation gravity mission in China, our group has been studying and developing a space-based PDH laser frequency stabilization system since 2013. We have constructed a prototype of a PDH laser frequency stabilization system [39] in which the FP cavity and its mode-matching optics are firmly integrated on an ultrastable monolithic optical bench using the hydroxide-catalysis bonding technique [40]. The digital control program realized on the field-programmable gate array (FPGA) platform was developed based on the dual-loop scanning and real-time analyzing algorithms [41]. Its functions include initial laser frequency calibration and automatic locking and relocking. The preliminary test shows that the laser frequency stability is better than 30 Hz/Hz$^{1/2}$ at a frequency band ranging from 0.7 Hz to 10 Hz.

In addition to the PDH method, the hyperfine transition of molecular iodine is another well-known absolute reference for laser frequency stabilization [42]. In this method, a 1064 nm laser is frequency doubled and locked to an absorbing hyperfine transition of iodine by the Doppler-free spectroscopy technique. In principle, laser frequency locking to the molecular
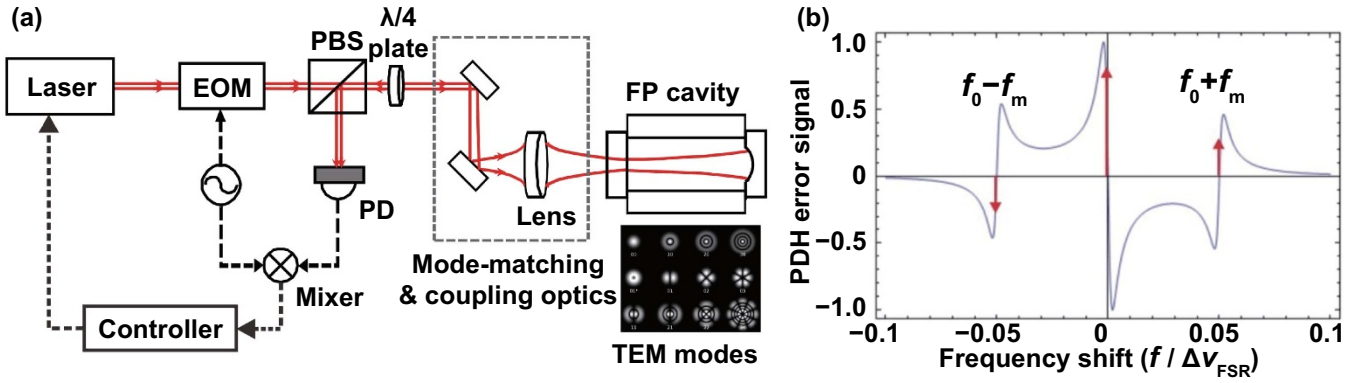
Figure 3. (a) Basic setup of the PDH laser frequency stabilization scheme: electro-optic modulator (EOM), polarized beam splitter (PBS), photodiode (PD), and (b) typical PDH dispersion curve of the error signal. The Bessel sidebands are marked on the curve.
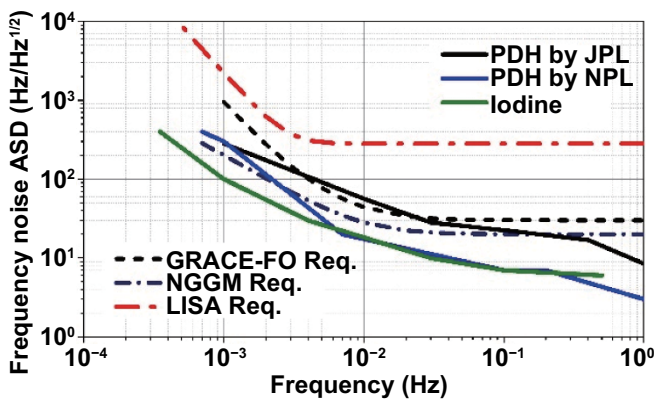

Figure 4. Laser frequency noise spectra, achieved by different experimental systems, in comparison with the space mission requirements. The solid black line refers to [30], the solid blue line refers to [31], and the solid green line refers to [32]. Recently, FP cavities with different designs of highly symmetric geometry, e.g. spherical [33, 34] and pyramidal [35] structures, are being studied, especially the mechanical supporting structures of the cavity which are improved by symmetrical distribution of mounting forces [36, 37].

iodine transition can offer an exact absolute frequency reference without thermal drift. It may simplify the initial heterodyne beat note acquisition process and thus has attracted more and more attention to study its potential applications for space-based laser interferometry [43, 44].

The best fractional frequency stability of the iodine-transition-based laser stabilization setup reaching the flicker floor at about 4×10^{-15} was realized in the laboratory [45] by a four-pass optical scheme and active control of residual amplitude modulation. The first flight-like absolute laser frequency reference for future space missions was developed based on a quasi-monolithic $^{127}I_2$ optical setup by the modulation transfer spectroscopy technique [32]. In this setup, the optical layouts are jointed into one integrated glass baseplate using the space-qualified adhesive bonding technique [46]; and the frequency stability achieved meets the requirements for LISA and NGGM, as shown by the solid green line in figure 4. The

improved setup based on this design was successfully flown on a sounding rocket in 2018 [47].

3. Precision phase measurement and weak-light phase locking

Weak-light phase-locking is the core technique for building an intersatellite transponder laser interferometer, and the residual phase noise of the phase-locked loop is determined by the precision of a phasemeter and the performance of the feedback control loop. In the following sections, we will introduce the working principle of a phasemeter and discuss the weak-light phase-locked loop.

3.1. Ultraprecision phasemeter

According to the requirements of space-based gravitational-wave detection missions, the noise level of phase measurement is $1 \sim 10$ μrad/Hz$^{1/2}$, corresponding to $0.1 \sim 1$ pm/Hz$^{1/2}$ for a laser wavelength of 1064 nm. For the GRACE-FO and NGGM missions, a measurement noise of about 1 mrad/Hz$^{1/2}$ will be enough to meet the requirements.

The output of the photodetector in a heterodyne laser interferometer is a beat-note signal, and the beat-note frequency is determined by the Doppler effect caused by the relative motion between two spacecraft. The information on gravitational waves or the Earth's gravity field is contained in the phase of this beat note. A phasemeter is used to measure the phase difference between the beat note and the reference signal provided by an onboard ultrastable oscillator (USO).

For spaceborne gravitational-wave detection missions, the typical requirements for a phasemeter are: (1) the resolution of phasemeter must achieve 10 μrad/$\sqrt{Hz}$ from 0.01 Hz to 1 Hz. (2) The phasemeter must have a large measurement range due to the Doppler frequency shift of $\sim$10 MHz caused by intersatellite relative motion. (3) The functions of automatic (laser) frequency acquisition and adjustable gain are needed because the amplitude and frequency of the beat note are unknown initially. Moreover, the phasemeter must provide a high data sampling rate for weak-light phase locking, which is discussed in the next section.

There are many types of phase measurement methods. The zero-crossing method was studied in [48–50]. The frequency of the measured signal can be as large as 20 MHz, and the resolution is about 0.01°. The major noise comes from the fluctuation of the reference voltage of the zero crossing.

The method based on phase-locked loop (PLL) is a closed-loop scheme for measuring phase. It has a high resolution and a large dynamic range. Since the frequency shift (caused by the Doppler effect) and the phase change (caused by the change in optical path length) of the beat note can be recorded, the displacement and the (intersatellite) relative speed can be obtained simultaneously. Therefore, the PLL-type phasemeter is the optimum method for intersatellite laser interferometry.

The research groups in the Joint Institute for Laboratory Astrophysics (JILA) [48–50], JPL [51–53], Germany Albert Einstein Institution (AEI) [54–59], Lulea University of Technology (LUT) [60], TianQin (Sun Yat-sen University and Huazhong University of Science and Technology) [61–63], and the National Microgravity Laboratory, Chinese Academy of Sciences (NML CAS) [64, 65], have gradually developed phasemeters since 2000. The method of zero crossing (JILA 2001, 2003, 2006, weak-light interferometer signal mixed to about 10 kHz) was replaced by the digital PLL method. For a signal frequency range of 1 mHz to 1 Hz, the noise level of the phasemeter has already achieved less than 1 μrad/Hz$^{1/2}$, which can meet the requirement of spaceborne gravitational-wave detection missions. Schwarze *et al* developed a picometer-level, stable, hexagonal optical bench to verify the LISA phasemeter [59]. However, the noise level of phase measurement at a low frequency band (0.1 $\sim$ 10 mHz) requires further study, especially in the case of weak light (100 pW) received and large heterodyne frequency shift (20 Hz s^{-1}). Data on the development and performance of precision phasemeters published thus far are summarized in figure 5.

The schematic diagram of a typical phasemeter based on the digital phase-locked loop (DPLL) algorithm is shown in figure 6. The analog input signal (i.e. the beat note of the heterodyne laser interferometer) is digitized by the sampling circuit that consists of a signal conditioning circuit (i.e. an antialias filter or an amplifier) and an analog-to-digital converter (ADC). This digitized signal is then multiplied by the sinusoidal signal generated by the numeric-controlled oscillator (NCO) to obtain the phase error. The signal of the phase error is then sent to a proportional-integral (PI) feedback controller, of which the control signal is used to keep phase synchronization between the NCO and the input beat note. To lock the phase of a signal with an unknown frequency, a frequency detector (counter) is used to perform automatic acquisition within a certain tracking range. Once the NCO is phase locked to the input signal, the frequency and the phase change of the NCO can be recorded, which correspond to the speed and the displacement of the measured target, respectively. All of the above processes can be realized either by using digital hardware (e.g. FPGA) or analog electronics.

3.2. Weak-light phase locking

Although a collimated laser beam is used in intersatellite laser interferometry, the beam size of the emitting laser propagating through a long intersatellite distance becomes much larger than that of the satellite. This is due to the divergence angle of laser beams determined by the diffraction limit and a very long propagation distance of about $10^5 \sim 10^6$ kilometers [66]. As a result, the light power received by the target satellite is very weak, and the power attenuation of the intersatellite laser beam is so serious that the typical scheme of a Michelson interferometer with only reflecting mirrors is not suitable to intersatellite laser interferometry. To solve this problem, an optical phase-locking technique is used, instead of a simple reflection. The optical phase-locked loop is able to lock the phase of the local (slave) laser to that of the light received. In this way, the light emitting from the slave laser has an identical phase to the received light but a much stronger light power.

The Doppler effect, caused by the relative motion between two satellites, is another issue needing to be considered. Although the satellites' orbits are analyzed and optimized to build up a stable triangle constellation, the relative motion between two satellites still varies periodically with a maximum speed of about 10 m s^{-1}, which will result in a Doppler frequency shift of 10 MHz [67, 68]. Therefore, a heterodyne phase-locked loop with an offset frequency of about $15 \sim 20$ MHz must be used. Moreover, the long-term stability and the low frequency residual noises of the weak-light phase locking are critical, especially for detecting low-frequency gravitational-wave signals.

The challenge of weak-light phase locking is to achieve ultrahigh precision phase measurements with interference signals of very small signal-to-noise ratio (SNR). Assume that the emitting laser power is 1 W, the intersatellite distance is 1 million kilometers, the diameter of telescope D is 30 cm, and the beam radius on the emitting telescope is $\omega_0 = 0.45D$. According to the far-field diffraction of a Gaussian laser beam $\theta_0 = \lambda/\pi\omega_0$ and the beam quality M$^2 = 1.2$, the divergence angle can be expressed as $\theta = $ M$^2\lambda/\pi\omega_0$ [69]. The beam diameter at the receiving spacecraft is $2L\theta \approx 6$ km; therefore, a telescope of 30 cm receives only 2.5 ppb of the laser power emitted. In addition to power attenuation due to long-distance propagation, the power loss of all optical components along the optical path of the interferometer must be taken into account, so that the effective light powers detected by photodetectors are even smaller [70].

Regarding the early development of weak-light phase locking, Enloe and Rodda [71] used a homodyne phase-locking technique, in 1965, to make two single frequency helium–neon (He–Ne) lasers to oscillate at exactly the same frequency with a residual phase difference of less than a third of one degree. After the 1990s, the optical phase-locked loop has been widely used in the areas of optical communication, quantum optics, cold atom physics, and laser interferometers [72–76]. This research established the foundation for the optical phase-locking technique. However, the research on weak-light phase locking faces new challenges, including
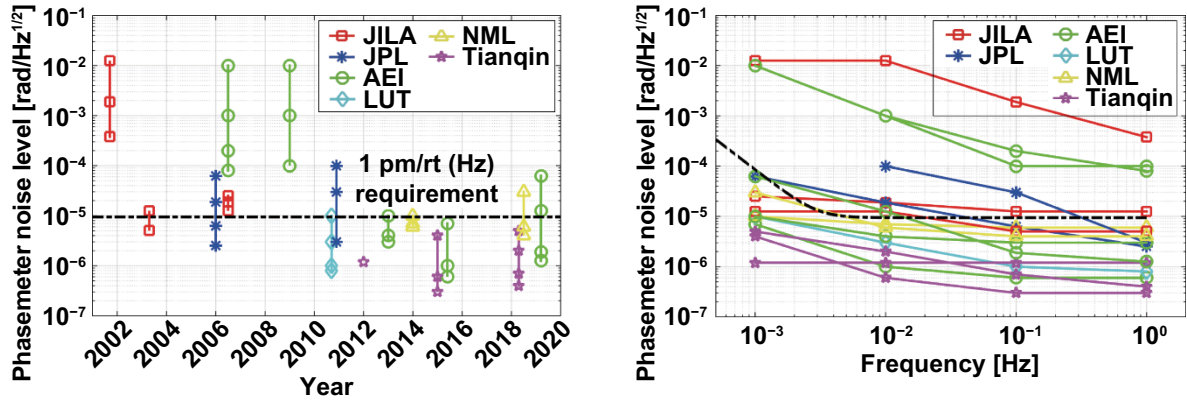
Figure 5. The development and performance of phasemeters for spaceborne gravitational-wave detection.
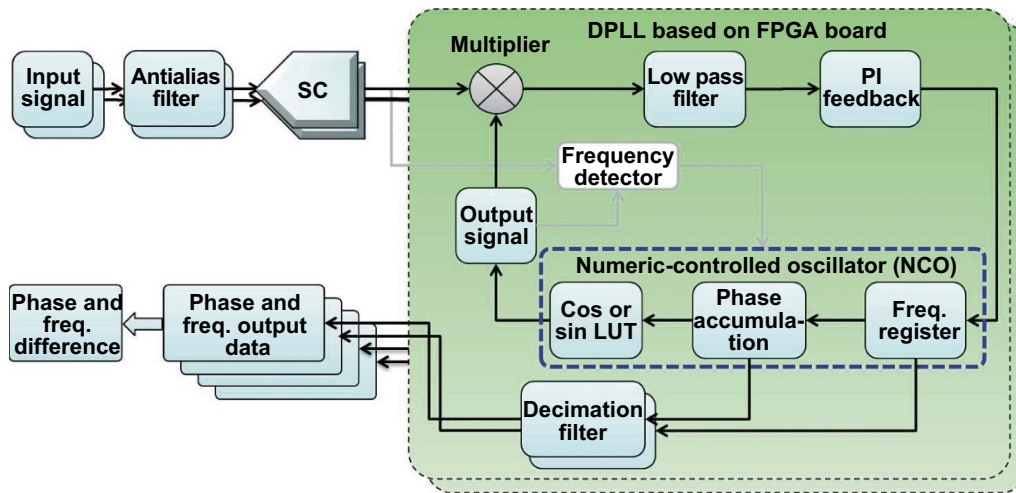

Figure 6. A schematic diagram of the frequency/phase measurement system based on DPLL: sampling circuit (SC); look-up table (LUT); and proportional-integral (PI) feedback controller.

quantum shot noise and phase noise at low frequency, ranging from 0.1 mHz to 1 Hz.

Liao *et al* demonstrated homodyne phase locking to 2 pW incoming weak light. The laser light was attenuated by using neutral density filters, and the balanced detection method was used to eliminate the laser intensity noise and improve the signal-to-noise ratio. The experimental results showed that the phase error was 290 mrad (rms) over a locking duration of 1.5 min [77].

Ye and Hall demonstrated a high-performance optical phase-locked loop between two continuous wave Nd:YAG lasers. The feedback system employed the laser's internal piezoelectric transducer (PZT) and an external acousto-optic modulator (AOM). The PZT (with the bandwidth of about 20 kHz) corrected slow but potentially large laser frequency drifts, and the AOM (with the bandwidth of about 200 kHz) eliminated fast frequency fluctuations. A residual phase noise of about 1 μrad was achieved, and the out-of-loop phase noise was approximately 0.6 μrad/Hz$^{1/2}$ at 1 Hz and above [78].

McNamara *et al* reported an experiment to evaluate a weak-light phase-locking scheme in which two independent, diode-pumped Nd:YAG NPRO lasers were locked together with a

15 MHz frequency offset. Using a weak light intensity of 17 nW, they obtained the smallest residual noise over the frequency range of 10 ∼ 800 Hz [79]. Based on this work, they improved the performance of weak-light phase locking for LISA in 2005. The experimental results showed that the residual phase noise of the slave laser reached the shot noise limit (0.13 mrad/Hz$^{1/2}$) above 0.4 Hz when the power of the weak light was attenuated down to 13 pW [66].

Diekmann *et al* implemented an analog optical phase-locked loop with an offset frequency of 20 MHz, in which the detected light powers of two lasers were 31 pW and 200 μW. The phase noise between two lasers was twice the shot noise limit down to 60 mHz, and the residual phase noise below 60 mHz mainly came from the analog electronics of the phasemeter. This paper gives some details on the noises generated by the photodetectors, such as the shot noise of the photodiode, the Johnson noise, and the equivalent current noise of the transimpedance amplifier [68].

Dick *et al* [80] and Francis *et al* [81] demonstrated weak-light phase locking with light powers down to 40 fW and 30 fW, respectively. In order to lock two lasers with such weak light powers, the parameters of the loop filter have to
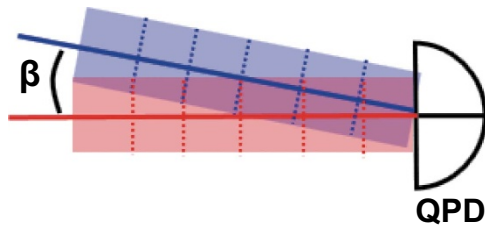
Figure 7. The basic principle of DWS.

Figure 8. A simplified schematic to show the basic principle of DPS.

be optimized to balance laser phase noise and shot noise, such that the cycle slip rate can be minimized.

The noises of weak-light phase locking come from three major components of a typical phase-locked loop: laser, phasemeter, and photodetector. The sources of laser noise include frequency fluctuation and photon number fluctuation (shot noise). Since the shot noise is a quantum noise limit, an optimized design of the phase-locked loop must ensure that the shot noise is dominant. In the presence of only shot noise, cycle slips in a phase-locked loop can be reduced to any desired level by reducing the loop bandwidth [82]. However, the loop bandwidth should be optimized when the laser frequency (phase) noise cannot be ignored.

The measurement noise of the phasemeter is caused by the sampling time jitter of the analog-to-digital convertor (ADC), the quantization error of the ADC, and the thermal drifts of some thermal-sensitive electronic components. The phase error caused by the sampling time jitter of the ADC can be reduced by using the pilot-tone correction technique [62, 63].

Principally speaking, reducing the in-loop noise requires a high control bandwidth. In contrast, reducing the out-loop noise requires a low control bandwidth. Therefore, the control bandwidth (or the loop gain) is a key parameter that should be optimized for weak-light phase locking. In addition, the loop (time) delay is another key parameter that should be carefully considered. According to the previous work [72], the control bandwidth should be determined by considering the loop delay and the laser frequency noise (i.e. the laser linewidth).

4. Intersatellite laser beam pointing control

As a Gaussian laser beam is used in intersatellite laser interferometry, most of the light power of the laser beam is concentrated within the Airy spot after a long (intersatellite) distance propagation. In case the laser beam axis is not exactly aligned with the line of sight of two laser-linked satellites, even the misalignment is just a bit larger than the Airy spot, the received light power will become very weak, so that an interference signal cannot be obtained due to a low signal-to-noise ratio. There are many factors that can influence the alignment of intersatellite laser beams, including satellites' attitude jitter, payload installation errors, laser beam jitter, and thermal-induced structural instability. Therefore, the intersatellite laser beam pointing control system must accomplish three processes, acquisition, tracking, and pointing of intersatellite laser beams, and that is why it is also called the acquisition/tracking/pointing (ATP) system. In addition, the
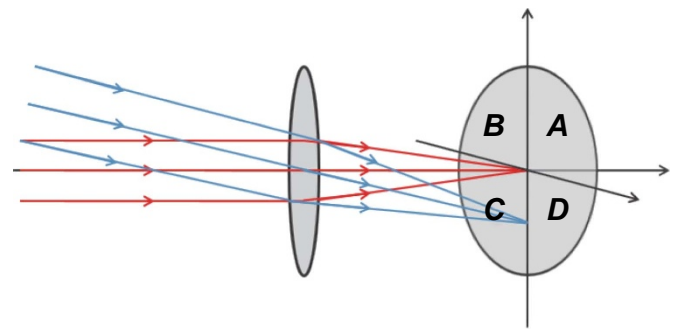
wave-front distortion coupling to the misalignment of the laser beam results in a displacement measurement error, which demands intersatellite pointing control with a precision of $1 \sim 10$ nrad/Hz$^{1/2}$ for gravitational-wave detection.

The ATP technology of intersatellite laser links was also used for intersatellite or ground-satellite laser communication [83, 84]. Typically, the initial misalignment offset between the line of sight and the beam axis is around 10^{-3} rad, primarily caused by the assembly tolerances and the vibration during launch. The common acquisition strategy is to scan the spatial uncertainty cone of the target satellite by using a fast steering mirror to adjust the emitting direction of the laser beam. When the detector on the received terminal (satellite) detects the optical signal, the laser beam of the received terminal is then adjusted to point back to the transmitted terminal accordingly. Today, most of the laser communication systems use a beacon light and a coarse/fine-composite ATP control system to perform acquisition and pointing of the laser link. For the transmitted terminal, thanks to high power and large-beam divergence of the beacon light, the number of scanning points for completely covering the uncertainty cone is greatly reduced, thus the acquisition time is reduced accordingly. For the received terminal, the charge-coupled devices (CCDs) are usually implemented as a measurement device of the beam position received because the wide field of view of the CCD helps to reduce the acquisition time. Once intersatellite beam acquisition is established, the quadrant photodiode (QPD) is used for tracking and ultrahigh precision pointing control.

There are some novel acquisition and pointing control schemes designed for space-based science missions, e.g. LISA [9], GRACE Follow-On [85], Space Advanced Gravity Measurements (SAGM) [86], etc. Differential wavefront sensing (DWS) is a well-known high-precision angle measurement technique [87]. A simplified schematic of the working principle is shown in figure 7. When the acquisition process is finished and the signal-to-noise ratio of the received signal meets the requirement for interference, the QPD outputs four interference beat-note signals by four quadrants. Each signal represents the phase detected by the corresponding quadrant of the QPD. Since the wave-front of the received light can be treated as a spherical wave-front due to a very long-distance propagation and the light beam detected by the QPD is only a

very small portion near the center of the beam axis, the wavefront detected by the QPD is almost flat. If the local laser beam is perfectly aligned with the received light, in principle, four phases of the interference signal detected by the QPD are identical. However, if the local beam is misaligned with the received beam, the phases output from the QPD are different; and the phase difference between two adjacent quadrants is proportional to the misalignment angle between the local beam and the received beam.

According to the above discussion, the displacement measurement can be realized by averaging four phases of the QPD output; and the misalignment angle can be obtained by calculating the phase difference between two adjacent quadrants of the QPD. The misalignment angle can be converted from the phase difference by multiplying a factor k, given by

$$k \approx \frac{16r}{3\lambda}, \tag{3}$$

where λ is the wavelength and r is the beam radius. The typical value of the conversion factor is approximately $10^3 \sim 10^4$ rad/rad. Thank to this large conversion factor, we can use the DWS technique to achieve an ultrahigh precision angle measurement.

For the acquisition process, there are five degrees of freedom (DoFs) which need to be calibrated, including two rotational DoFs for each satellite and one DoF for the laser frequency difference between the master and the slave lasers.

The schemes of intersatellite laser beam acquisitions must be designed specifically to meet the unique requirements of different space missions. In the LISA mission, the acquisition uncertainty cone is estimated to be 15.2 μrad; and the beam divergence angle is about 1.43 μrad [88]. It is obvious that the uncertainty cone is larger than the beam divergence angle. The field of view of the QPD is 1 μrad, which is also smaller than the beam divergence angle, so a series of steps must be taken to accomplish the acquisition. First, the offset between the star tracker's axis and the associated CCD center is measured by observing stars for each satellite; and the two satellites adjust their attitudes to point to each other. The transmitted beam of the master satellite scans the uncertainty cone. Meanwhile, the slave satellite turns off its local laser and searches for the corresponding signal by the acquisition CCD until the CCD gets the signal. Then the slave satellite adjusts its attitude until the received beam is located at the center of the QPD. In turn, the slave and the master satellites reverse roles and repeat the same acquisition procedures to accomplish the first step of the acquisition.

In addition to the spatial scan, the frequency scan must be performed by tuning the slave laser until the beat frequency enters the detection bandwidth of the QPD, so that the interference signal is detectable by the QPD. Once the slave laser has been tuned to have a proper frequency, the intersatellite laser beam acquisition is complete.

The definition of operational procedure, the design of the acquisition control system, and the development of an end-to-end constellation simulator for the LISA mission have been proposed; and the simulation results show that the total acquisition time is about 70 min. In the GRACE-FO mission [89],

the QPD and signal processing hardware are used to perform intersatellite laser link acquisition. The radius of the uncertainty cone is about 3 mrad, and the initial offset of laser frequency between the master and the slave lasers is estimated to be 1 GHz. The initial laser link acquisition is achieved by scanning over five DoFs. The master laser beam scans with a fast Lissajous pattern, while the slave laser beam scans with a slower hexagonal pattern. At the same time, the slave laser frequency is tuned slowly during the spatial scan. The information about the orientation of the fast steering mirror and the temperature of the slave laser are downlinked to the ground station for obtaining the pointing angles and the laser frequency, respectively; and the amplitude of the interference signal obtained by using the fast Fourier transform (FFT) peak detection algorithm is sequentially recorded on each satellite. This process usually takes several hours. After initial acquisition, the spatial uncertainty cones and the frequency difference can be reduced to 300 μrad and 20 MHz, respectively. Finally, the DWS base automatic acquisition achieves the fast, precise pointing control to meet the requirements of space missions. The on-orbit results of GRACE-FO show that the acquisition scheme works well, and the initial acquisition scan takes about 8.5 h. The reacquisition takes less than 5 min [17].

In order to reduce the acquisition time, an alternative acquisition scheme based on the laser power detection is proposed [90]. The laser beam emitting from the master satellite is intensity modulated and scans the uncertainty cone of the slave satellite. When the scan of the master satellite is finished, then the slave satellite starts scanning. Once both satellites have finished scanning, the scan data (i.e. received light intensity with coordinates) are sent to ground station for further data processing. According to the coordinates at which the modulated signal strength is maximum, the pointing angles of the laser beams can be determined and adjusted. The frequency scan is performed, and the heterodyne signal is detected by the QPD such that the DWS can be used to do fine adjustments of the laser beam pointing. The numerical simulation results show that the total acquisition time can be reduced from several hours to 160 s.

For the next-generation gravity measurement mission proposed in China [91], we are studying a new intersatellite laser beam acquisition scheme. The acquisition schemes discussed above use one-way scanning for either the uncertainty cone of the slave satellite or the uncertainty cone of the master satellite. If both satellites can scan at the same time, then the acquisition time can be even shorter.

The basic idea is to modulate the power of the laser beams emitting from the master satellite and the slave satellite with different modulation frequencies so that the laser beams from different satellites can be demodulated and identified independently. In this way, scanning by the two satellites can be started simultaneously. In addition, the misalignment angle of the laser beam can be determined by the powers detected by four quadrants of the QPD because an inclined laser beam will be focused at different positions on the QPD such that the powers detected by different quadrants of the QPD are different. This detection of the misalignment angle is called the differential power sensing (DPS) method [92]. Figure 8 shows the

simplified schematic of the working principle of DPS. After passing through the focus lens, the positions of spots detected by the QPD depend on the incident angles of the laser beams.

Instead of waiting for scanning of the entire uncertainty cone to be complete, the local laser beam is adjusted immediately to align with the beam axis of the received laser light when one of the satellites detects the signal with a power above the default threshold. Within a short time delay propagating through intersatellite distance, the other satellite also receives enough power. Then two satellites can perform fine adjustments to laser beam pointing control based on DPS. The simulation experiment demonstrates that the residual noise of pointing jitter is less than 30 μrad, and the average acquisition time is less than 10 s for a scanning range of 1 mrad radius with a success rate of more than 99%.

Once the spatial acquisition is complete, the frequency of the slave laser is tuned until the heterodyne signal is obtained. Finally, the DWS technique can be used in the case of ultrahigh precision pointing control when a pointing jitter down to 10^{-9} rad is needed.

5. Conclusion

Precision measurement provides a strong support to the development of advanced manufacturing. Laser interferometry, as a typical example of precision measurement technique, has many important applications in manufacturing. In this paper, we review the development and latest research on intersatellite laser interferometry in which the measurement conditions and measurement precision are required to be pushed to extreme limits. We expect that some matured key technologies of intersatellite laser interferometry will be used for extreme manufacturing in the near future.

Acknowledgment

ORCID iD

Hsien-Chi Yeh ⓘ https://orcid.org/0000-0001-8947-2052

References

[1] LIGO 2020 (www.ligo.caltech.edu/)
[2] LISA 2020 (www.lisamission.org/)
[3] Ni W T 2013 Astrod-gw: overview and progress *Int. J. Mod. Phys.* D **22** 1341004
[4] Luo J *et al* 2016 TianQin: a space-borne gravitational wave detector *Class. Quantum Grav.* **33** 035010
[5] Hu W R and Wu Y L 2017 The Taiji program in space for gravitational wave physics and the nature of gravity *Natl Sci. Rev.* **4** 685–6
[6] Kawamura S *et al* 2006 The Japanese space gravitational wave antenna—DECIGO *Class. Quantum Grav.* **23** S125–31
[7] Roberts M, Taylor P and Gill P 1999 Laser linewidth at the sub-hertz level *NPL Report* CLM 8 National Physics Laboratory
[8] Sullivan D B, Allan D W, Howe D A and Walls F L 1990 *Characterization of Clocks and Oscillators* (Boulder, CO: National Institute of Standards and Technology)
[9] Danzmann K and Rüdiger A 2003 LISA technology—concept, status, prospects *Class. Quantum Grav.* **20** S1–S9
[10] Danzmann K and Prince T 2011 LISA Assessment Study *Report* (Yellow Book) ESA/SRE(2011)3 European Space Agency
[11] Sheard B S, Gray M B, McClelland D E and Shaddock D A 2003 Laser frequency stabilization by locking to a LISA arm *Phys. Lett.* A **320** 9–21
[12] Shaddock D A, Ware B, Spero R E and Vallisneri M 2004 Postprocessed time-delay interferometry for LISA *Phys. Rev.* D **70** 081101
[13] Kane T J and Byer R L 1985 Monolithic, unidirectional single-mode Nd:YAG ring laser *Opt. Lett.* **10** 65–67
[14] Hildebrand U, Lange R and Smutny B 2006 Fiber-optic components for the laser communication terminal on TerraSAR-X 16 PPT online (https://photonics.gsfc.nasa.gov/)
[15] Muehlnikel G, Kämpfner H, Heine F, Zech H, Troendle D, Meyer R and Phillip-May S 2012 The alphasat GEO laser communication terminal flight acceptance tests *Proc. Int. Conf. on Space Optical Systems and Applications* (*Ajaccio, Corsica, France*)
[16] Armano M *et al* 2016 Sub-femto-*g* free fall for space-based gravitational wave observatories: LISA pathfinder results *Phys. Rev. Lett.* **116** 231101
[17] Abich K *et al* 2019 In-orbit performance of the GRACE follow-on laser ranging interferometer *Phys. Rev. Lett.* **123** 031101
[18] Freitag I, Tünnermann A and Welling H 1995 Power scaling of diode-pumped monolithic Nd:YAG lasers to output powers of several watts *Opt. Commun.* **115** 511–5
[19] Tröbs M 2005 *Laser Development and Stabilization for the Spaceborne Interferometric Gravitational Wave Detector LISA* (Hannover: Universität Hannover)
[20] Tröbs M, d'Arcio L, Heinzel G and Danzmann K 2009 Frequency stabilization and actuator characterization of an ytterbium-doped distributed-feedback fiber laser for LISA *J. Opt. Soc. Am.* B **26** 1137–40
[21] Numata K, Chen J R and Camp J 2010 Fiber laser development for LISA *J. Phys. Conf. Ser.* **228** 012043
[22] Numata K and Camp J 2012 Experimental performance of a single-mode ytterbium-doped fiber ring laser with intracavity modulator *Laser Phys. Lett.* **9** 575–80
[23] Numata K, Camp J, Krainak M A and Stolpner L 2010 Performance of planar-waveguide external cavity laser for precision measurements *Opt. Express* **18** 22781–8
[24] Numata K and Camp J 2012 Precision laser development for interferometric space missions NGO, SGO, and GRACE follow-on *J. Phys. Conf. Ser.* **363** 012054
[25] Camp J, Numata K and Krainak M 2017 Progress and plans for a US laser system for LISA *J. Phys. Conf. Ser.* **840** 012013
[26] Schwander T *et al* 2017 New 808 nm high power laser diode pump module for space applications *Proc. SPIE* **10567** 105671C
[27] Traub M, Plum H D, Hoffmann H D and Schwander T 2007 Spaceborne fiber coupled diode laser pump modules for intersatellite communications *Proc. SPIE* **6736** 673618
[28] Drever R W P, Hall J L, Kowalski F V, Hough J, Ford G M, Munley A J and Ward H 1983 Laser phase and frequency stabilization using an optical resonator *Appl. Phys.* B **31** 97–105
[29] Black E D 2001 An introduction to Pound–Drever–Hall laser frequency stabilization *Am. J. Phys.* **69** 79–87

[30] Pierce R *et al* 2012 Stabilized lasers for space applications: a high TRL optical cavity reference system *Proc. 2012 Conf. on Lasers and Electro-Optics* (San Jose, CA: IEEE) pp 1–2

[31] Nicklaus K *et al* 2017 High stability laser for next generation gravity missions *Proc. SPIE* **10563** 105632T

[32] Döringshoff K, Schuldt T, Kovalchuk E V, Stühler J, Braxmaier C and Peters A 2017 A flight-like absolute optical frequency reference based on iodine for laser systems at 1064 nm *Appl. Phys.* B **123** 183

[33] Leibrandt D R, Bergquist J C and Rosenband T 2013 Cavity-stabilized laser with acceleration sensitivity below 10^{-12} g^{-1} *Phys. Rev.* A **87** 023829

[34] Leibrandt D R, Thorpe M J, Notcutt M, Drullinger R E, Rosenband T and Bergquist J C 2011 Spherical reference cavities for frequency stabilization of lasers in non-laboratory environments *Opt. Express* **19** 3471–82

[35] Didier A *et al* 2018 Ultracompact reference ultralow expansion glass cavity *Appl. Opt.* **57** 6470–3

[36] Świerad D *et al* 2016 Ultra-stable clock laser system development towards space applications *Sci. Rep.* **6** 33973

[37] Chen Q F, Nevsky A, Cardace M, Schiller S, Legero T, Häfner S, Uhde A and Sterr U 2014 A compact, robust, and transportable ultra-stable laser with a fractional frequency instability of 1×10^{-15} *Rev. Sci. Instrum.* **85** 113107

[38] Webster S and Gill P 2011 Force-insensitive optical cavity *Opt. Lett.* **36** 3572–4

[39] Luo Y X, Li H Y, Liang Y R, Duan H Z, Zhang J Y and Yeh H-C 2016 A preliminary prototype of laser frequency stabilization for spaceborne interferometry missions *Proc. 2016 European Frequency and Time Forum* (York: IEEE) pp 1–4

[40] Elliffe E J *et al* 2005 Hydroxide-catalysis bonding for stable optical systems for space *Class. Quantum Grav.* **22** S257–67

[41] Luo Y X, Li H Y and Yeh H C 2016 Note: digital laser frequency auto-locking for inter-satellite laser ranging *Rev. Sci. Instrum.* **87** 056105

[42] Arie A, Schiller S, Gustafson E K and Byer R L 1992 Absolute frequency stabilization of diode-laser-pumped Nd:YAG lasers to hyperfine transitions in molecular iodine *Opt. Lett.* **17** 1204–6

[43] Nakagawa K, Shimo-oku A, Nakagawa K and Musha M 2016 Developments of highly frequency and intensity stabilized lasers for space gravitational wave detector decigo/pre-decigo *Proc. SPIE* **10562** 105620H

[44] Acef O and Du Burck F 2019 Nd:YAG laser frequency stabilized for space applications *Proc. SPIE* **10565** 1056568

[45] Zang E J, Cao J P, Li Y, Li C Y, Deng Y K and Gao C Q 2007 Realization of four-pass I_2 absorption cell in 532-nm optical frequency standard *IEEE Trans. Instrum. Meas.* **56** 673–6

[46] Gohlke M, Schuldt T, Döringshoff K, Peters A, Johann U, Weise D and Braxmaier C 2015 Adhesive bonding for optical metrology systems in space applications *J. Phys. Conf. Ser.* **610** 012039

[47] Schkolnik V *et al* 2017 JOKARUS-design of a compact optical iodine frequency reference for a sounding rocket mission *EPJ Quantum Technol.* **4** 9

[48] Jennrich O, Stebbins R T, Bender P L and Pollack S 2001 Demonstration of the LISA phase measurement principle *Class. Quantum Grav.* **18** 4159–64

[49] Pollack S E, Jennrich O, Stebbins R T and Bender P 2003 Status of LISA phase measurement work in the US *Class. Quantum Grav.* **20** S193–9

[50] Pollack S E and Stebbins R T 2006 Demonstration of the zero-crossing phasemeter with a LISA test-bed interferometer *Class. Quantum Grav.* **23** 4189–200

[51] Ware B, Folkner W M, Shaddock D, Spero R, Halverson P, Harris I and Rogstad T 2006 Phase measurement system for inter-spacecraft laser metrology *Proc. 2006 Earth Science Technology Conf.* (Maryland, MD: NASA)

[52] Hsu M T, Littler I C M, Shaddock D A, Herrmann J, Warrington R B and Gray M B 2010 Subpicometer length measurement using heterodyne laser interferometry and all-digital rf phase meters *Opt. Lett.* **35** 4202–4

[53] De Vine G, Rabeling D S, Slagmolen B J J, Lam T T Y, Chua S, Wuchenich D M, McClelland D E and Shaddock D A 2009 Picometer level displacement metrology with digitally enhanced heterodyne interferometry *Opt. Express* **17** 828–37

[54] Wand V, Guzmán F, Heinzel G and Danzmann K 2006 LISA phasemeter development *AIP Conf. Proc.* **873** 689–96

[55] Bykov I, Delgado J E, Marín A F G, Heinzel G and Danzmann K 2009 LISA phasemeter development: advanced prototyping *J. Phys. Conf. Ser.* **154** 012017

[56] Gerberding O, Sheard B, Bykov I, Kullmann J, Delgado J J E, Danzmann K and Heinzel G 2013 Phasemeter core for intersatellite laser heterodyne interferometry: modelling, simulations and experiments *Class. Quantum Grav.* **30** 235029

[57] Schwarze T S, Gerberding O, Cervantes F G, Heinzel G and Danzmann K 2014 Advanced phasemeter for deep phase modulation interferometry *Opt. Express* **22** 18214–23

[58] Gerberding O *et al* 2015 Readout for intersatellite laser interferometry: measuring low frequency phase fluctuations of high-frequency signals with microradian precision *Rev. Sci. Instrum.* **86** 074501

[59] Schwarze T S, Barranco G F, Penkert D, Kaufer M, Gerberding O and Heinzel G 2019 Picometer-stable hexagonal optical bench to verify LISA phase extraction linearity and precision *Phys. Rev. Lett.* **122** 081104

[60] Burnett M C 2010 Development of an ultra-precise digital phasemeter for the LISA gravitational wave detector *Thesis* Lulea University of Technology

[61] Liang Y R, Duan H Z, Yeh H C and Luo J 2012 Fundamental limits on the digital phase measurement method based on cross-correlation analysis *Rev. Sci. Instrum.* **83** 095110

[62] Liang Y R, Duan H Z, Xiao X L, Wei B B and Yeh H C 2015 Note: inter-satellite laser range-rate measurement by using digital phase locked loop *Rev. Sci. Instrum.* **86** 016106

[63] Liang Y R 2018 Note: a new method for directly reducing the sampling jitter noise of the digital phasemeter *Rev. Sci. Instrum.* **89** 036106

[64] Liu H S, Dong Y H, Li Y Q, Luo Z R and Jin G 2014 The evaluation of phasemeter prototype performance for the space gravitational waves detection *Rev. Sci. Instrum.* **85** 024503

[65] Liu H S, Luo Z R and Jin G 2018 The development of phasemeter for Taiji space gravitational wave detection *Microgravity Sci. Technol.* **30** 775–81

[66] McNamara P W 2005 Weak-light phase locking for LISA *Class. Quantum Grav.* **22** S243–7

[67] Danzmann K 2017 *LISA—Laser Interferometer Space Antenna: A Proposal in Response to the ESA Call for L3 Mission Concepts* (Hannover: Leibniz Universitat Hannover and Max Planck Institute for Gravitational Physics)

[68] Diekmann C, Steier F, Sheard B, Heinzel G and Danzmann K 2009 Analog phase lock between two lasers at LISA power levels *J. Phys. Conf. Ser.* **154** 012020

[69] Photonics Enclypedia 2020 (www.rp-photonics.com/beam_divergence.html)

[70] Bender P L 2000 LISA–Laser interferometer space antenna: a cornerstone mission for the observation of gravitational waves Report ESA-SCI(2000)11 European Space Agency

[71] Enloe L H and Rodda J L 1965 Laser phase-locked loop *Proc. IEEE* **53** 165–6

[72] Ramos R T and Seeds A J 1990 Delay, linewidth and bandwidth limitations in optical phase-locked loop design *Electron. Lett.* **26** 389–91

[73] Win M Z, Chen C C and Scholtz R A 1991 Optical phase-locked loop for free-space laser communications with heterodyne detection *Proc. SPIE* **1417** 42–52

[74] Santarelli G, Clairon A, Lea S N and Tino G M 1994 Heterodyne optical phase-locking of extended-cavity semiconductor lasers at 9 GHz *Opt. Commun.* **104** 339–44

[75] Le Gouët J, Kim J, Bourassin-Bouchet C, Lours M, Landragin A and dos Santos F P 2009 Wide bandwidth phase-locked diode laser with an intra-cavity electro-optic modulator *Opt. Commun.* **282** 977–80

[76] Xu Z X, Zhang X, Huang K K and Lu X H 2012 A digital optical phase-locked loop for diode lasers based on field programmable gate array *Rev. Sci. Instrum.* **83** 093104

[77] Liao A C, Ni W T and Shy J T 2002 Pico-watt and femto-watt weak-light phase locking *Int. J. Mod. Phys.* D **11** 1075–85

[78] Ye J and Hall J L 1999 Optical phase locking in the microradian domain: potential applications to NASA spaceborne optical measurements *Opt. Lett.* **24** 1838–40

[79] McNamara P W, Ward H and Hough J 1998 Laser phase-locking techniques for LISA: experimental status *AIP Conf. Proc.* **456** 143–7

[80] Dick G J, Tu M R, Strekalov M D, Birnbaum K and Yu N 2008 Optimal phase lock at femtowatt power levels for coherent optical deep-space transponder *IPN Prog. Rep.* **42** 1–17

[81] Francis S P, Lam T T Y, McKenzie K, Sutton A J, Ward R L, McClelland D E and Shaddock D A 2014 Weak-light phase tracking with a low cycle slip rate *Opt. Lett.* **39** 5251–4

[82] Viterbi A J 1966 Phase-locked-loop behavior in the presence of noise *Principles of Coherent Communication* (New York: McGraw-Hill) pp 77–120

[83] Tolker-Nielsen T and Oppenhauser G 2002 In-orbit test result of an operational optical intersatellite link between ARTEMIS and SPOT4, SILEX *Proc. SPIE* **4635** 1–15

[84] Jono T *et al* 2006 OICETS on-orbit laser communication experiments *Proc. SPIE* **6105** 610503

[85] Sheard B S, Heinzel G, Danzmann K, Shaddock D A, Klipstein W M and Folkner W M 2012 Intersatellite laser ranging instrument for the GRACE follow-on mission *J. Geod.* **86** 1083–95

[86] Yeh H C, Yan Q Z, Liang Y R, Wang Y and Luo J 2011 Intersatellite laser ranging with homodyne optical phase locking for Space Advanced Gravity Measurements mission *Rev. Sci. Instrum.* **82** 044501

[87] Heinzel G *et al* 2004 The LTP interferometer and phasemeter *Class. Quantum Grav.* **21** S581–7

[88] Cirillo F and Gath P F 2009 Control system design for the constellation acquisition phase of the LISA mission *J. Phys. Conf. Ser.* **154** 012014

[89] Wuchenich D M R *et al* 2014 Laser link acquisition demonstration for the GRACE Follow-On mission *Opt. Express* **22** 11351–66

[90] Luo Z R, Wang Q L, Mahrdt C, Goerth A and Heinzel G 2017 Possible alternative acquisition scheme for the gravity recovery and climate experiment follow-on-type mission *Appl. Opt.* **56** 1495–500

[91] Zhang J Y, Ming M, Jiang Y Z, Duan H Z and Yeh H C 2018 Inter-satellite laser link acquisition with dual-way scanning for Space Advanced Gravity Measurements mission *Rev. Sci. Instrum.* **89** 064501

[92] Manojlović L M 2011 Quadrant photodetector sensitivity *Appl. Opt.* **50** 3461–9